Pixel Level Fusion of Panchromatic and Multispectral Images Based on Correspondence Analysis

Halil I. Cakir and Siamak Khorram

Abstract

A pixel level data fusion approach based on correspondence analysis (CA) is introduced for high spatial and spectral resolution satellite data. Principal component analysis (PCA) is a well-known multivariate data analysis and fusion technique in the remote sensing community. Related to PCA but a more recent multivariate technique, correspondence analysis, is applied to fuse panchromatic data with multispectral data in order to improve the quality of the final fused image. In the CA-based fusion approach, fusion takes place in the last component as opposed to the first component of the PCA-based approach. This new approach is then quantitatively compared to the PCA fusion approach using Landsat ETM+, QuickBird, and two Ikonos (with and without dynamic range adjustment) test imagery. The new approach provided an excellent spectral accuracy when synthesizing images from multispectral and high spatial resolution panchromatic imagery.

Introduction

Many Earth observing satellites (sensors) are providing increasingly high-spatial resolution multispectral data. However, two major factors limit a remote sensing sensor's ability to collect high spatial resolution, multi-spectral data (Zhang, 2004). First, the incoming radiation energy to sensor is limited by optics size. Second, the data volume to be collected and stored by the sensor increases exponentially with higher spatial resolutions. Thus, satellites, such as QuickBird and Ikonos, bundle a 4:1 ratio of a high-resolution panchromatic band and lower resolution multi-spectral bands in order to support both color and best spatial resolution, while minimizing on-board data handling needs.

The on-ground fusion of panchromatic and multi-spectral bands may provide an improved product to users, dependent upon the ability of the fusion technique to accurately reproduce a synthetic (fused) imagery from a multispectral imagery while improving the spatial resolution. Hence, many fusion techniques are developed to integrate both panchromatic and multispectral data in order to increase the spatial resolution of the former (e.g., Cliche *et al.*, 1985; Price, 1987; Welch and Ehlers, 1987; Chavez *et al.*, 1991; Ehlers, 1991; Shettigara, 1992; Yesou *et al.*, 1993; Zhou *et al.*, 1998; Liu and Moore, 1998; Zhang, 1999; Lemeshewsky, 1999; Ranchin and Wald, 2000; Laben, and Brower, 2000; Ranchin *et al.*, 2003; Cakir and Khorram, 2003; Chen *et al.*, 2005)

A critical consideration is how to integrate spatial information present in the panchromatic image but missing from the low-resolution multispectral data. Many techniques transform multispectral data from color space to a new space in order to have at least one component highly similar to panchromatic data such as the principal component analysis (PCA) or intensity-hue-saturation (IHS)-based techniques. By substituting this component with panchromatic data and then performing inverse transformation to original color space, a new multispectral image with the spatial resolution of panchromatic data is achieved. However, accurate production of the synthetic image is dependent upon the spectral equality of the substituted component and the panchromatic band (Švab and OŠtir, 2006). Thus, panchromatic data is preprocessed (i.e., histogram matched) before the substitution in order to increase the similarity to the substituted component. In general, transformation methods that result in a component more similar to the panchromatic band do better in terms of the spectral accuracy of the synthesized images. Some recent studies have focused on this aspect to improve the fusion process such as the new modified-IHS proposed by Siddiqui (2003) and FFT-enhanced IHS method by Ling *et al.* (2007).

One of the most widely used fusion approaches is based on the principal component analysis of the images. PCA is a multivariate statistical technique that deals with the internal structure of matrices. It breaks down or partitions a resemblance matrix into a set of orthogonal (perpendicular) axes or components. Traditionally, this matrix consists of variance-covariances or correlations (If a correlation matrix is used for principal component calculation, it is also known as "factor analysis" or "standardized principal components."). Each PCA axis corresponds to an eigenvalue of the matrix. Given an image with *n*-number of bands, *n*-number of principal components can be calculated. PCA is useful for image encoding, image data compressing, image enhancement, digital change detection, multitemporal dimensionality, and image fusion (Pohl and Genderen, 1998). Some image fusion applications of the PCA method in the literature are given by Chavez *et al.* (1991).

A more recent multivariate method, correspondence analysis (CA) was developed independently by several authors. An algebraic derivation of CA is often accredited to

Center for Earth Observation, North Carolina State University, Campus Box 7106, Raleigh, NC 27695 (halil_cakir@ncsu.edu).

Photogrammetric Engineering & Remote Sensing
Vol. 74, No. 2, February 2008, pp. 183–192.

0099-1112/08/7402–0000/$3.00/0
© 2008 American Society for Photogrammetry and Remote Sensing

Hirschfield (1935) who developed a formulation of the correlation between the rows and columns of a two-way contingency table (Beh, 2004). For the development, history, and more information of the technique, readers are referred to Hill (1974), Greenacre (1984), Benzécri (1992), and Beh (2004). The term "correspondence analysis" is a translation of the French "analyse factorielle des correspondances."

Correspondence analysis can be applied to data tables other than contingency tables as long as the elements of a table to be analyzed are dimensionally homogenous (i.e., same physical units, so that they can be added) and non-negative (so that they can be transformed into probabilities or proportions). The difference between PCA and the CA is that CA preserves the chi-square (χ^2) distance when computing the association between bands (Carr and Matanawi, 1999). In PCA, the distance among objects, in both the multidimensional space of original descriptors and the reduced space, are calculated using Euclidean distances. Most of the time, the last CA component is omitted from the analyzing procedure because the last eigenvalue is insignificant or small. However, this could be a valuable asset in the data fusion process in carrying over the spatial details from the high spectral resolution imagery into the multispectral imagery.

Although it is very well known to ecologists (Legendre and Legendre, 1998; Gauch, 1982), correspondence analysis is rarely explored in the remote sensing community. Carr and Matanawi (1999) introduced CA for principal component transformations of multispectral and hyperspectral imagery. Later, Cakir *et al.* (2006) successfully applied it to change detection.

In the following sections, a new pixel level data fusion process based on correspondence analysis is introduced and applied to satellite imagery.

Methods

The PCA Approach in Pixel Level Data Fusion

The PCA approach in pixel level data fusion is a five-step fusion process:

1. Geometric registration of the images to be fused.
2. Calculation of the principal components, or principal component transformation of the multispectral imagery.
3. Modification of the high spatial resolution imagery (usually a panchromatic image) to match with the first principal component of the multispectral imagery.
4. Replacement of the first component image with the high spatial resolution imagery.
5. Inverse transformation of the principal components image to original space.

After the multispectral imagery is transformed into principal components, high spatial resolution imagery (single band image) is usually stretched to have the same variance and average as the first principal component (PC1). Then, the stretched high spatial resolution image replaces the PC1 image of the transformed multispectral imagery. The assumption behind this is that the first principal component carries the information common to all bands and is approximately equal to the high spatial resolution image. The rest of the principal components contain the spectral information unique to each band (Chavez and Kwarteng, 1989). Thus, replacing PC1 with high spatial resolution imagery should not (theoretically) effect the spectral accuracy of the fused product.

At the final step of the fusion process, the new data set is transformed back to its original data space after the replacement of PC1

The Correspondence Analysis (CA) Approach in Pixel Level Data Fusion

The first step of PCA transformation is the standardization of the data matrix that termed "*row centering.*" In the CA approach, the data table (X) is transformed into a table of contributions to the Pearson chi-square statistic. First, pixel (x_{ij}) values are converted to proportions (p_{ij}) by dividing each pixel (x_{ij}) value by the sum (x_{++}) of all pixels in data set. The result is a new data set of proportions (table Q), and the size is (rxc). Row weight p_{i+} is equal to x_{i+}/x_{++}, where x_{i+} is the sum of values in row i. Vector $[p_{i+}]$ is of size (r). Column weight p_{+j} is equal to x_{+j}/x_{++}, where x_{+j} is the sum of values in column j. Vector $[p_{+j}]$ is of size (c).

The Pearson chi-square statistic, χ^2_p, is a sum of squared χ_{ij} values; χ_{ij} values computed for every cell ij of the contingency table:

$$\chi_{ij} = \frac{o_{ij} - E_{ij}}{\sqrt{E_{ij}}} = \sqrt{x_{++}}\left[\frac{p_{ij} - p_{i+}p_{+j}}{\sqrt{p_{i+}p_{+j}}}\right]. \quad (1)$$

If we use q_{ij} values instead of χ_{ij} values, so that $q_{ij} = \chi_{ij}/\sqrt{x_{++}}$, eigenvalues will be smaller than or equal to 1 which is more convenient. We used the q_{ij} values to form matrix $\overline{Q}_{rxc}$ which is:

$$\overline{Q}_{rxc} = \left[q_{ij}\right] = \left[\frac{p_{ij} - p_{i+}p_{+j}}{\sqrt{p_{i+}p_{+j}}}\right] \quad (2)$$

After this point, the calculation of eigenvalues and the eigenvectors is similar to the PCA method. Matrix U produced by:

$$U_{cxc} = \overline{Q}^T_{cxr}\,\overline{Q}_{rxc} \quad (3)$$

which is similar to covariance matrix of PCA. Multispectral data are then transformed into the component space using the matrix of eigenvectors.

A difference between CA and PCA fusion approach is the substitution of the last component with the high spatial resolution imagery as opposed to the substitution of the first component in the PCA. Two methods can be used in this part of the CA fusion process. The first is the substitution of the last component with panchromatic band, which is stretched to have same range and variance with the last CA component. Second is the injection of details from the panchromatic band into the last component. Spatial details can be represented as the ratios of pixel values at the highest spatial resolution to the pixel values at the lower resolutions of the same imagery. Similar to a procedure explained by Liu (2000), spatial details can be injected into the last component by using the formula:

$$CA_{SimComp} = \frac{Pan_{High}}{Pan_{mean}} * CA_{LastComp} \quad (4)$$

where $CA_{SimComp}$ is the new simulated last component image with the spatial resolution of Pan_{High} which is the high spatial resolution panchromatic image. Pan_{Mean} is the image with local mean values of Pan_{High} over neighborhoods equivalent to footprints of $CA_{LastComp}$ image pixels. Noting that Pan_{Mean} can be calculated either by block averaging pixels within the footprints of the low spatial resolution image pixels (Liu and Moore, 1998), or using smoothing convolution filters (Liu, 2000). Block averaging is used in this study for Pan_{Mean} so that values are calculated once for each lower resolution pixel block as an average of the high spatial resolution pixels within the block.

Finally, the components image is transformed back to the original image space using the inverse matrix of eigenvectors.

Quality Assessment

A variety of quality assessment procedures have been reported in the literature for pan-sharpened images. There is a general consensus that more work is needed before a universal procedure can be defined (Aiazzi *et al.*, 2002). The lack of availability of truth (reference) images with the same spatial resolution as the fused image makes quality assessment particularly difficult (Wald *et al.*, 1997). There are two methods commonly used to mitigate this problem. One method is to degrade the fused image back to the original image resolution prior to assessment. Another method involves the degradation of both pan and multispectral imagery by the same factor prior to fusion. In both ways, the original image becomes the reference image to compare it to either degraded fused image, or the fused image synthesized from lower resolutions. With these two methods, a number of parameters can be calculated to measure the accuracy of the fusion, including any bias in the mean, correlation coefficients, standard deviation of the difference image from the reference (original) image, difference between the variance of reference image and that of fused image, and the root mean square error (RMSE) (Wald *et al.*, 1997; Ranchin and Wald, 2000; Aiazzi *et al.*, 2002; Ranchin *et al.*, 2003). Most often, these parameters are reported as percentages of the means of each reference image band, except in the case of the difference of the variances, which is reported as a percentage to the reference image variance. For the RMSE however, it would be better to report relative root mean square error (R-RMSE) instead of RMSE as the percentage of the reference image band mean.

The relative root mean square error (R-RMSE) standardizes the RMSE computed per pixel to the *true* value observed in that pixel location. The resulting R-RMSE value is expressed as a percent, and represents the standard variation of the fusion. The R-RMSE assigns equal weight to any overestimation or underestimation of the statistic (Kroll and Stedinger, 1996). R-RMSE for multispectral images for a given band of k is expressed as:

$$R-RMSE_k = \sqrt{\frac{\sum_{i=1}^{N}\left(\frac{DN_{fused(k),i} - DN_{original(k),i}}{DN_{original(k)}}\right)^2}{N}} \quad (5)$$

where, DN is the pixel value, and i is the pixel number in band k.

Based on RMSE, a dimensionless global relative error of fusion (ERGAS) proposed by Wald (2002) is given as:

$$ERGAS = 100 \cdot \frac{h}{l}\sqrt{\frac{1}{K}\sum_{k=1}^{K}\left(\frac{RMSE(k)}{\mu_o(k)}\right)^2} \quad (6)$$

where, h/l is the ratio between pixel sizes pan and MS images (e.g., 1:4 for Ikonos and QuickBird, and 1:2 for Landsat-7), $\mu_o(k)$ is the mean of the k^{th} band, and the K is the number of bands.

Wang and Bovik (2002) introduced a universal objective image quality measure called the Q index. For a given reference image x and fused image y to be tested, the Q index value can be calculated as:

$$Q = \frac{4\sigma_{xy}\cdot\mu_{o(x)}\cdot\mu_{o(y)}}{(\sigma_x^2+\sigma_y^2)\left[(\mu_{o(x)})^2+(\mu_{o(x)})^2\right]} \quad (7)$$

where σ_{xy} is the covariance between reference and fused image, $\mu_{o(x)}$ and $\mu_{o(y)}$ are the means, and σ_x^2 and σ_y^2 the variances of the reference and fused images respectively.

The dynamic range of Q is $[-1, 1]$. The formula of Q can be rewritten as a product of three components:

$$Q = \frac{\sigma_{xy}}{\sigma_x\sigma_y}\cdot\frac{2\mu_{o(x)}\mu_{o(y)}}{(\mu_{o(x)})^2+(\mu_{o(y)})^2}\cdot\frac{2\sigma_x\sigma_y}{\sigma_x^2\sigma_y^2}. \quad (8)$$

The first component is the correlation coefficient between the reference and fused images, and has a value range of $[-1, 1]$. The second component's value range is $[0, 1]$, which is sensitive to any bias in the mean of the fused image with respect to the reference image mean. The third component's value range is also $[0, 1]$. It is sensitive to changes in variances between the reference and fused image, and can be viewed as the measure of contrast similarity between them. An ideal Q value of 1 can be achieved when the fused and reference image values are equal to each other on a pixel-by-pixel basis.

One final remark on quality assessment procedures is that the selected degradation technique itself can influence the quality of the assessment. Wald *et al.* (1997) reports that this effect can be minimized by the selection of a proper degradation procedure among many available ones such as simple averaging, wavelets, cubic convolution, bi-cubic spline, and methods using Modulation Transfer Function (MTF) of the sensor. For example, the consequences of MTF filtering are proofed by Aiazzi *et al.* (2006). It should be noted that the choice of degradation method should be clearly reported in the quality assessment of the fusion method. Currently, it was omitted in most studies. In this study, simple averaging is used as the degradation process for all methods.

Application

Four images are tested in this study. These images are an 8-bit Landsat-7 ETM+ imagery of California's San Francisco Bay (SFB) area (excluding thermal infrared band), an 11-bit QuickBird imagery of North Raleigh (Figure 1), North Carolina, and two 11-bit Ikonos images with and without dynamic range adjustment (DRA)[1]. The Landsat scene was acquired on 07 July 1999 and covers approximately 22,705 km^2 (5,134 × 4,914 multispectral pixels). The QuickBird imagery was acquired in summer of 2002. Multispectral image dimensions are 2,940 pixels by 1,540 pixels (approximately 26 km^2). Ikonos imagery of coastal Georgia with DRA off has dimensions of 2,048 pixels by 2,048 pixels (approximately 67 km^2). Ikonos imagery of Wilson, North Carolina, with DRA on was acquired in 2002 and has image dimensions of 512 pixels by 512 pixels (4.19 km^2).

Two CA fusion methods, one with the replacement of last component with stretched pan image and one with the injection of details into last component using Equation 4, were implemented and tested using the test images listed above. Results were compared to two equivalent PCA based methods (one with the replacement of the first component with the stretched pan image and another with the injection of details into the first component using Equation 4.)

Visual comparisons revealed that all the fused images inherited high spatial information from the panchromatic image very well. Both CA and PCA approaches with detail injection to components method provided sharp synthetic

[1] A DRA algorithm attempts to optimize the most significant portion of the data distribution or histogram, usually at the expense of the least significant portions. This stretching leads to changes in radiometric accuracy and can be problematic for pansharpening.

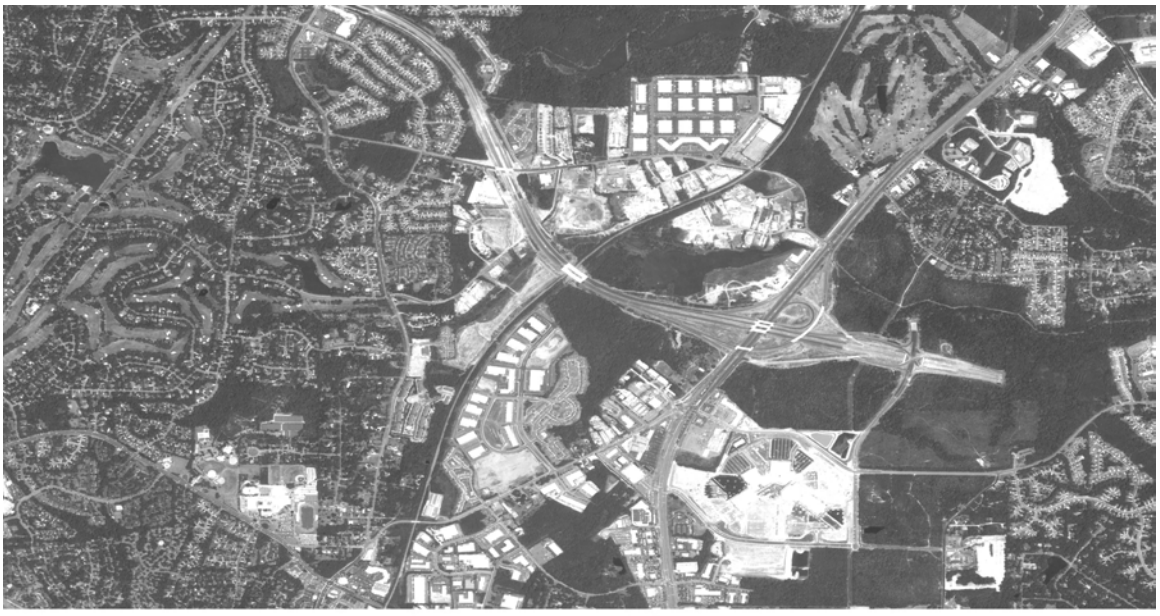

(a)

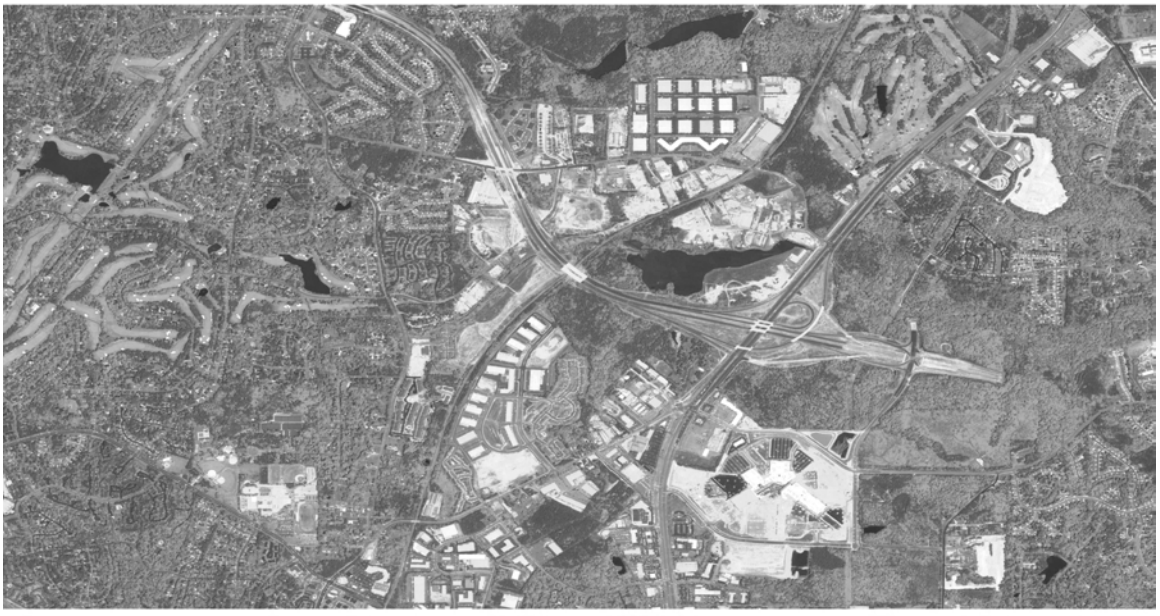

(b)

Figure 1. True color (a) and false color (b) display of QuickBird test imagery over Raleigh, North Carolina. A color version of this figure available on the ASPRS website: **www.asprs.org**.

images with good color balance as seen from the Figure 2a and 2b and Figure 3a and 3b for QuickBird imagery. However, color distortion was evident for the PCA-based stretched PAN substitution method in some test images especially for the QuickBird data (Figure 2c and 2d and Figure 3c and 3d). For all displays, same look-up (contrast) tables are used as suggested by Wald *et al.*, (1997).

In order to evaluate the quality of the fusion quantitatively, test images were spatially degraded to lower resolutions. Landsat data was degraded by a factor of two (into 30- and 60-meter spatial resolution for PAN and MS, respectively). QuickBird and Ikonos data were degraded by a factor of four. As previously discussed, fusion from lower resolutions results in a fused product with the same spatial resolution as the original input multispectral image (30-meter for Landsat, 2.44-meter for QuickBird, and 4-meter for Ikonos). This enables the direct comparison between the fused and original, which becomes a reference image for comparative evaluations of the accuracy of the fusion process.

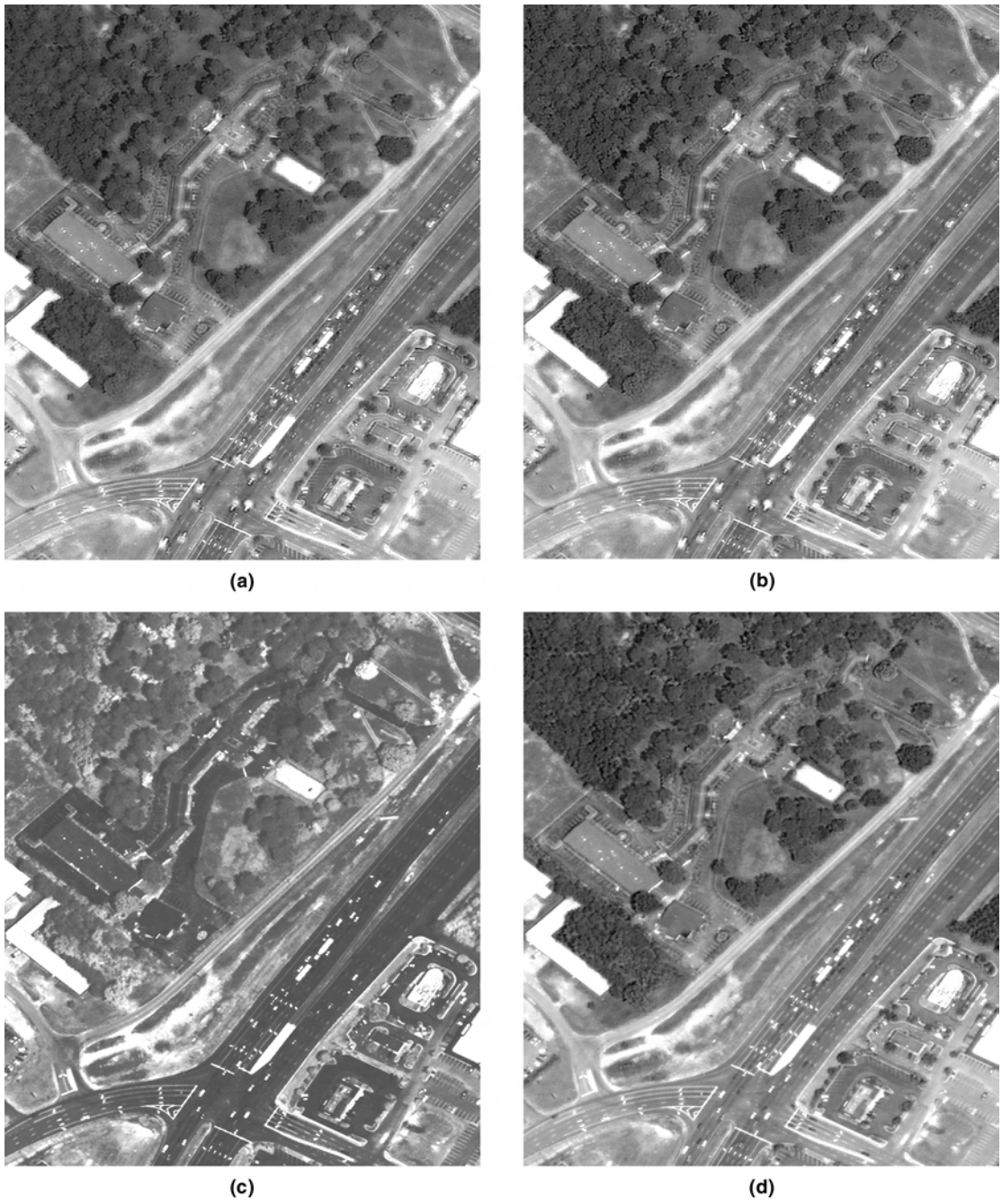

Figure 2. True color display of the fused images for the QuickBird data at the 61 cm resolution. Only a subset of the whole image is shown: (a) PCA fusion with detail injection, (b) CA fusion with detail injection, (c) PCA fusion with stretched panchromatic band substitution, and (d) CA fusion with stretched panchromatic band substitution. A color version of this figure available on the ASPRS website: **www.asprs.org**.

Mean bias (μ_{Diff}) values, standard deviations of the differences (σ_{Diff}), differences in variances, and R-RMS errors are reported in Tables 1, 2, 3, and 4, respectively, for all test images and fusion methods. Interestingly, based on these parameters and test images, CA-based methods performed better in infrared bands while PCA-based methods performed better in the blue band. One possible explanation is that in PCA, the distances between objects, in both the multidimensional space of the original descriptors and the reduced space, is proportional to the statistical covariance. Since the blue band usually has the highest covariance with other bands (for the data types used in this study), PCA applies more emphasis to blue band and less to the infrared band, which usually has the lowest covariance

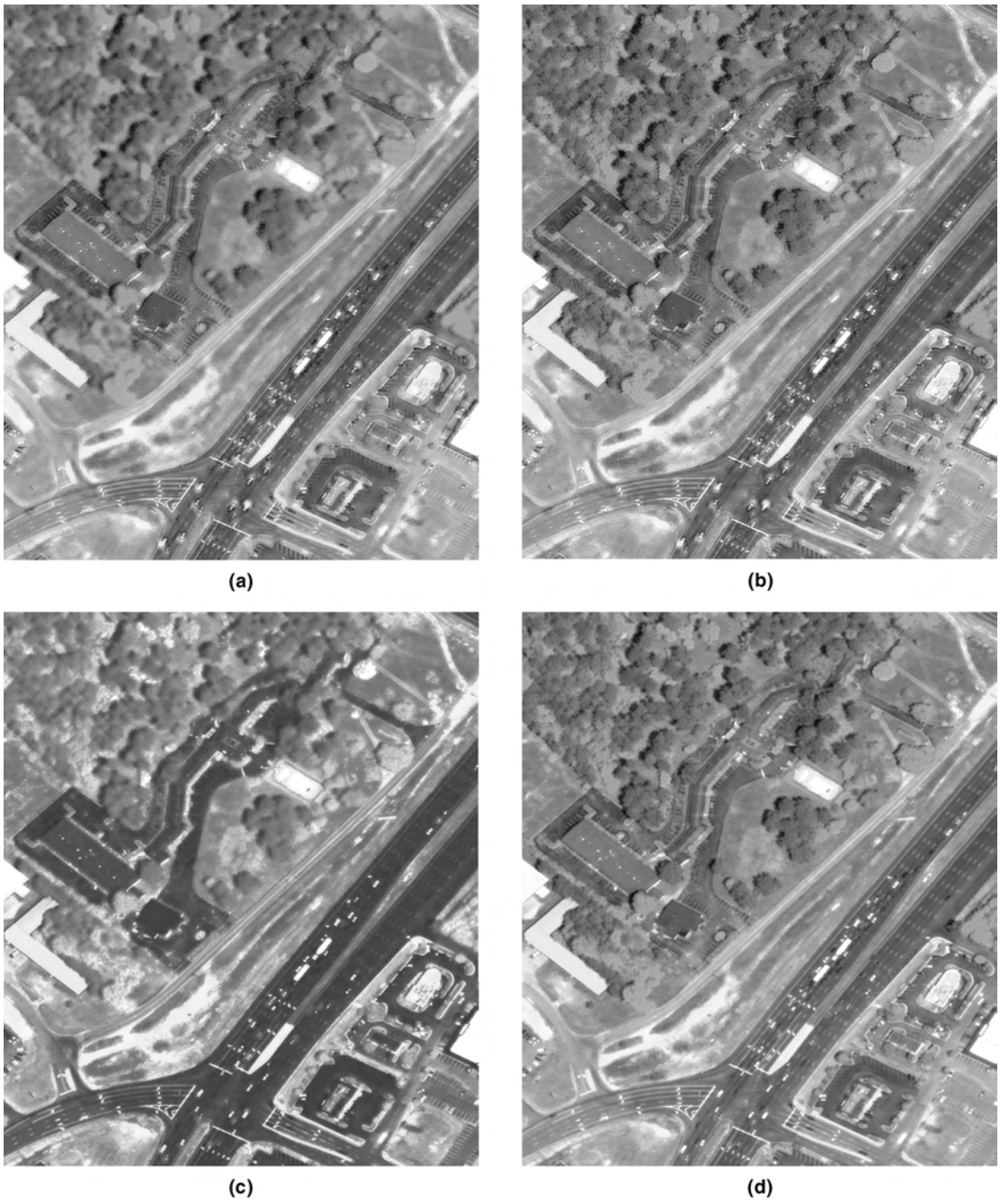

Figure 3. False color display of the fused images for the QuickBird data at the 61 cm resolution. Only a subset of the whole image is shown: (a) PCA fusion with detail injection, (b) CA fusion with detail injection, (c) PCA fusion with stretched panchromatic band substitution, and (d) CA fusion with stretched panchromatic band substitution. A color version of this figure available on the ASPRS website: **www.asprs.org**.

values with other bands. On the other hand, CA gives more emphasis to dissimilarity. Since the infrared bands are the most dissimilar bands to other bands, CA puts more weight on these bands.

ERGAS values which represent global error for each image are reported in Table 5. Wald (2002) suggests that an ERGAS value less than three represents satisfactory quality or better. Based on this suggestion, both CA and PCA based methods with detail injection did very well in terms of fusion quality for QuickBird and Ikonos with DRA-off imagery. They also performed satisfactorily for the Landsat imagery. However, all methods performed relatively poorly for the Ikonos-Wilson imagery. This was especially true for band 4 where spectral and radiometric composition of the data were altered with the DRA procedure in order to optimize the most significant portion of

TABLE 1. MEAN BIASES (μ_{Diff}) AND THEIR RELATIVE VALUES TO ORIGINAL IMAGE MEANS (μ_o). BEST RESULTS ARE GIVEN IN BOLD

		CA-Detail injection		CA – Stretched PAN substitution		PCA-Detail injection		PCA – Stretched PAN substitution	
		μ_{Diff}	μ_{Diff} as % to μ_o	μ_{Diff}	μ_{Diff} as % to μ_o	μ_{Diff}	μ_{Diff} s % to μ_o	μ_{Diff}	μ_{Diff} as % to μ_o
Landsat	Band1	−0.25	−0.31%	0.30	0.37%	**−0.12**	**−0.14%**	0.60	0.75%
	Band2	−0.24	−0.36%	0.26	0.39%	**−0.14**	**−0.22%**	0.81	1.22%
	Band3	−0.25	−0.33%	0.28	0.38%	**−0.20**	**−0.27%**	1.65	2.20%
	Band4	−0.27	−0.24%	0.38	0.34%	**−0.07**	**−0.07%**	0.42	0.38%
	Band5	−0.27	−0.24%	0.38	0.34%	**−0.21**	**−0.18%**	2.12	1.88%
	Band7	−0.24	−0.34%	0.27	0.38%	**−0.20**	**−0.28%**	1.55	2.16%
QuickBird	Band1	**−0.23**	**−0.07%**	2.58	0.83%	1.00	0.32%	2.74	0.88%
	Band2	**−0.25**	**−0.06%**	3.13	0.70%	1.59	0.35%	4.84	1.08%
	Band3	**−0.23**	**−0.08%**	2.49	0.85%	1.22	0.42%	4.51	1.55%
	Band4	**−0.25**	**−0.04%**	3.99	0.56%	1.52	0.21%	0.85	0.12%
Ikonos Coastal	Band1	**−0.36**	**−0.09%**	3.07	0.73%	−0.97	−0.23%	2.13	0.51%
	Band2	**−0.35**	**−0.09%**	3.03	0.74%	−1.64	−0.40%	2.91	0.71%
	Band3	**−0.33**	**−0.11%**	2.60	0.85%	−1.77	−0.58%	2.83	0.92%
	Band4	**−0.35**	**−0.08%**	3.18	0.72%	−2.92	−0.66%	4.62	1.04%
Ikonos Wilson	Band1	**−1.46**	**−0.25%**	4.69	0.80%	7.84	1.33%	9.64	1.64%
	Band2	**−1.50**	**−0.21%**	5.24	0.74%	8.77	1.24%	10.45	1.48%
	Band3	**−1.50**	**−0.22%**	5.18	0.75%	8.71	1.25%	10.46	1.51%
	Band4	−48.43	−7.42%	−41.72	−6.39%	**−41.28**	**−6.32%**	−41.75	−6.39%

TABLE 2. STANDARD DEVIATIONS OF THE DIFFERENCE IMAGES (σ_{Diff}) AND THEIR RELATIVE VALUES TO ORIGINAL IMAGE MEANS (μ_o). BEST RESULTS ARE GIVEN IN BOLD

		CA-Detail injection		CA – Stretched PAN substitution		PCA-Detail injection		PCA – Stretched PAN substitution	
		σ_{Diff}	σ_{Diff} as % to μ_o	σ_{Diff}	σ_{Diff} as % to μ_o	σ_{Diff}	σ_{Diff} as % to μ_o	σ_{Diff}	σ_{Diff} as % to μ_o
Landsat	**Band1**	**4.07**	**5.04%**	**9.62**	**11.92%**	3.44	4.26%	**7.14**	**8.84%**
	Band2	**3.62**	**5.46%**	**8.65**	**13.03%**	3.39	5.10%	**8.93**	**13.45%**
	Band3	5.00	6.67%	**9.67**	**12.90%**	**5.55**	**7.40%**	**17.02**	**22.69%**
	Band4	4.55	4.07%	**10.99**	**9.82%**	**4.85**	**4.34%**	**6.36**	**5.69%**
	Band5	7.64	6.75%	**12.66**	**11.18%**	**8.38**	**7.40%**	**21.78**	**19.23%**
	Band7	6.18	8.61%	**10.21**	**14.22%**	**6.51**	**9.06%**	**16.49**	**22.95%**
	AVERAGE	5.18	6.10%	**10.30**	**12.18%**	**5.35**	**6.26%**	**12.95**	**15.48%**
QuickBird	**Band1**	**38.36**	**12.34%**	**31.97**	**10.28%**	26.15	8.41%	**66.20**	**21.29%**
	Band2	**42.70**	**9.53%**	**36.31**	**8.10%**	41.08	9.16%	**119.94**	**26.75%**
	Band3	**38.22**	**13.11%**	**33.90**	**11.62%**	38.21	13.10%	**120.98**	**41.48%**
	Band4	59.95	8.49%	**63.00**	**8.92%**	**98.36**	**13.92%**	**105.58**	**14.94%**
	AVERAGE	44.81	10.86%	**41.29**	**38.92%**	**50.95**	**11.15%**	**103.17**	**26.12%**
Ikonos – Coastal (DRA off)	**Band1**	**23.11**	**5.52%**	**22.84**	**5.45%**	14.77	3.53%	**26.32**	**6.28%**
	Band2	21.19	5.17%	**21.64**	**5.28%**	**24.92**	**6.09%**	**28.68**	**7.00%**
	Band3	21.21	6.92%	**21.89**	**7.14%**	**26.91**	**8.77%**	**26.16**	**8.53%**
	Band4	32.74	7.36%	**35.31**	**7.93%**	**44.51**	**10.00%**	**41.74**	**9.38%**
	AVERAGE	24.57	6.24%	**25.42**	**6.45%**	**27.78**	**7.10%**	**30.72**	**7.80%**
Ikonos – Wilson	**Band1**	142.74	24.27%	**154.00**	**26.19%**	**165.53**	**28.15%**	**291.78**	**49.62%**
	Band2	131.61	18.63%	**148.78**	**21.06%**	**153.72**	**21.76%**	**267.05**	**37.81%**
	Band3	145.37	20.94%	**161.55**	**23.28%**	**166.98**	**24.06%**	**282.55**	**40.71%**
	Band4	222.07	34.00%	**236.00**	**36.14%**	**344.08**	**52.69%**	**361.73**	**55.39%**
	AVERAGE	160.45	24.46%	**175.08**	**26.67%**	**207.58**	**31.66%**	**300.78**	**45.88%**

the data distribution or histogram, usually at the expense of the least significant portions. Overall, CA-based methods were better than PCA-based methods in terms of ERGAS value for the test images.

For a final quantitative quality measure, Q values for individual bands and averages for entire MS images are reported in Table 6 for all methods and test images. This quality test also showed that PCA-based methods performed very well in blue bands while CA based methods were performing better in infrared bands. However, it also showed an overall trend that CA outperformed PCA in most of the cases.

TABLE 3. DIFFERENCES IN VARIANCES BETWEEN ORIGINAL (REFERENCE) AND FUSED IMAGES AS PERCENTAGE OF THE ORIGINAL VARIANCES ($\sigma^2_{original} - \sigma^2_{fused}$). BEST RESULTS ARE GIVEN IN BOLD

		CA-Detail injection	CA – Stretched PAN substitution	PCA-Detail injection	PCA – Stretched PAN substitution
Landsat	**Band1**	**−15.78%**	**−14.80%**	**−6.60%**	−4.54%
	Band2	**−8.94%**	0.54%	**−6.47%**	**−8.72%**
	Band3	**−1.59%**	**15.91%**	**−6.55%**	−0.02%
	Band4	**−8.32%**	**−88.13%**	−2.46%	**−33.90%**
	Band5	0.85%	**21.85%**	**−5.35%**	**8.50%**
	Band7	1.08%	**26.95%**	**−4.01%**	**18.75%**
QuickBird	**Band 1**	**−27.15%**	**8.78%**	**−8.53%**	−6.63%
	Band 2	**−7.90%**	**14.30%**	−6.90%	**−12.24%**
	Band 3	−2.92%	**13.63%**	**−5.78%**	**−6.46%**
	Band 4	2.50%	**11.12%**	**15.70%**	**29.91%**
Ikonos – Coastal (DRA off)	**Band 1**	**−22.28%**	**11.56%**	**−18.95%**	−5.69%
	Band 2	**−5.57%**	**14.09%**	**−23.54%**	3.95%
	Band 3	−0.51%	**14.82%**	**−23.79%**	**7.49%**
	Band 4	3.97%	**4.92%**	**−25.46%**	**4.63%**
Ikonos – Wilson (DRA on)	**Band 1**	−1.29%	**39.22%**	**−11.80%**	**10.57%**
	Band 2	**−5.74%**	**39.83%**	**−10.40%**	5.37%
	Band 3	−1.20%	**43.59%**	**−7.72%**	**12.00%**
	Band 4	**34.83%**	27.32%	**51.68%**	**64.19%**

TABLE 4. RELATIVE ROOT MEAN SQUARED ERRORS (R-RMSE) BETWEEN ORIGINAL AND FUSED MS IMAGES. BEST RESULTS ARE GIVEN IN BOLD

		CA-Detail injection	CA – Stretched PAN substitution	PCA-Detail injection	PCA – Stretched PAN substitution
Landsat	Band1	4.80%	12.75%	**4.06%**	9.39%
	Band2	5.26%	14.67%	**4.84%**	15.16%
	Band3	**7.34%**	18.08%	7.67%	32.10%
	Band4	**4.12%**	9.88%	4.33%	5.75%
	Band5	**7.40%**	13.83%	7.83%	24.06%
	Band7	**9.95%**	20.70%	10.01%	33.82%
	AVERAGE	**6.46%**	14.98%	**6.46%**	20.05%
QuickBird	Band1	12.86%	10.13%	**8.28%**	22.26%
	Band2	10.50%	**8.16%**	9.16%	28.87%
	Band3	21.49%	18.96%	**17.50%**	53.39%
	Band4	**9.68%**	10.71%	16.94%	18.36%
	AVERAGE	13.63%	**11.99%**	12.97%	30.72%
Ikonos – Coastal (DRA off)	Band1	5.24%	**4.99%**	**3.16%**	6.11%
	Band2	4.66%	**4.43%**	5.29%	6.53%
	Band3	6.27%	**6.06%**	7.75%	7.88%
	Band4	**7.51%**	8.50%	9.18%	8.83%
	AVERAGE	**5.92%**	6.00%	6.35%	7.34%
Ikonos – Wilson (DRA on)	Band1	52.31%	66.68%	**48.22%**	107.94%
	Band2	**59.56%**	82.20%	62.04%	82.56%
	Band3	86.72%	119.33%	**85.21%**	115.45%
	Band4	**337.03%**	337.90%	482.21%	518.84%
	AVERAGE	**133.91%**	151.53%	169.42%	206.19%

TABLE 5. ERGAS VALUES FOR ALL TEST IMAGES AND METHODS. BEST RESULTS ARE GIVEN IN BOLD

	CA-Detail injection	CA – Stretched PAN substitution	PCA-Detail injection	PCA – Stretched PAN substitution
Landsat	3.14	**6.13**	**3.26**	**8.46**
QuickBird	**2.76**	2.46	**2.85**	**6.98**
Ikonos – Coastal (DRA off)	1.58	**1.65**	**1.88**	**1.98**
Ikonos – Wilson (DRA on)	6.36	**6.87**	**8.54**	**11.64**

TABLE 6. Q-STATISTICS FOR ALL METHODS. IDEAL VALUE IS 1. BEST RESULTS ARE GIVEN IN BOLD

		CA-Detail injection	CA – Stretched PAN substitution	PCA-Detail injection	PCA – Stretched PAN substitution
Landsat	$\mathbf{Q_{Band\ 1}}$	**0.95**	**0.71**	0.96	**0.83**
	$\mathbf{Q_{Band\ 2}}$	**0.97**	**0.84**	0.98	**0.83**
	$\mathbf{Q_{Band\ 3}}$	0.98	**0.93**	**0.98**	**0.81**
	$\mathbf{Q_{Band\ 4}}$	0.98	**0.90**	**0.97**	**0.96**
	$\mathbf{Q_{Band\ 5}}$	0.98	**0.93**	**0.97**	**0.80**
	$\mathbf{Q_{Band\ 7}}$	0.97	**0.92**	0.97	**0.79**
	$Q_{Average}$	0.97	**0.87**	0.97	**0.84**
QuickBird	$\mathbf{Q_{band1}}$	**0.91**	**0.92**	0.95	**0.70**
	$\mathbf{Q_{band2}}$	**0.96**	0.97	**0.97**	**0.73**
	$\mathbf{Q_{band3}}$	**0.97**	0.98	**0.97**	**0.72**
	$\mathbf{Q_{band4}}$	0.96	**0.95**	**0.89**	**0.86**
	$Q_{Average}$	**0.95**	0.96	**0.95**	**0.75**
Ikonos – Coastal	$\mathbf{Q_{band1}}$	**0.93**	**0.92**	0.97	**0.90**
	$\mathbf{Q_{band2}}$	0.97	0.97	**0.96**	**0.95**
	$\mathbf{Q_{band3}}$	0.98	**0.97**	**0.96**	**0.96**
	$\mathbf{Q_{band4}}$	0.98	**0.97**	**0.96**	**0.96**
	$Q_{Average}$	0.97	**0.96**	**0.96**	**0.94**
Ikonos – Wilson	$\mathbf{Q_{band1}}$	0.91	**0.87**	**0.89**	**0.61**
	$\mathbf{Q_{band2}}$	0.92	**0.87**	**0.89**	**0.65**
	$\mathbf{Q_{band3}}$	0.91	**0.85**	**0.88**	**0.63**
	$\mathbf{Q_{band4}}$	0.83	**0.81**	**0.54**	**0.45**
	$Q_{Average}$	0.89	**0.85**	**0.80**	**0.58**

Conclusions

In this paper, correspondence analysis (CA) was introduced to the fusion of high spectral resolution imagery with high spatial resolution imagery at the pixel level. For most of the study images, the CA procedure described here performed equally well or better compared to PCA-based methods. Although both procedures are very similar to each other in terms of structure, the CA procedure differs from PCA in two distinctive ways: first, CA preserves the chi-square (χ^2) distance when computing the association between bands. Second, fusion takes place in the last component as opposed to the first component in PCA. Because the last component has almost zero original image variance in the CA-based methods (in most cases), theoretically altering the last component will not as greatly affect the spectral content of the original image. In PCA however, by replacing the first component with the panchromatic image, most of the original image variance is altered (the first component represents the most of the original image variance). This could be acceptable if the panchromatic imagery is highly correlated to first principal component. Depending on the scene and the contents of the imagery, the correlation between the panchromatic image and the first PCA component could be high and the PCA method may perform well but it is not the case at all times.

CA and PCA seemed to be complimentary fusion methods where each performed well in different bands. For the study images, CA-based methods performed better in infrared bands while PCA-based methods performed better in blue bands. Depending upon the need of the user; this could be an interesting trait that informs the selection of the appropriate fusion procedure for a particular application. However, given the fact that the infrared band usually carries more information than the blue band, a CA-based approach might have a slight edge over PCA in most applications.

One final remark is that both CA and PCA fusion results were dramatically improved when spatial details from panchromatic bands were injected into the last (as in CA) or first (as in PCA) components rather then substituting with a stretched panchromatic band. This suggests that even further improvements are possible to both CA- and PCA-based methods if better injection methods can be implemented.

References

Aiazzi, B., L. Alparone, and S. Baronti, 2002. Context driven fusion of high spatial and spectral resolution images based on oversampled multiresolution analysis, *IEEE Transactions on Geoscience and Remote Sensing*, 40(10):2300–2312.

Aiazzi, B., L. Alparone, S. Baronti, A. Garzelli, and M. Selva, 2006. MTF-tailored multiscale fusion of high resolution MS and Pan imagery, *Photogrammetric Engineering & Remote Sensing*, 72(5):591–596.

Beh, E.J., 2004. Simple correspondence analysis: A bibliographic review, *International Statistical Review*, 72(2):257–284

Benzécri, J.P., 1992.*Correspondence Analysis Handbook*, New York, Marcel Dekker.

Cakir, H.I., and S. Khorram, 2003. Fusion of high spatial resolution imagery with high spectral resolution imagery using multiresolution approach, *Proceedings of the ASPRS Annual Conference*, May, Anchorage, Alaska, unpaginated CD-ROM.

Cakir, H.I., S. Khorram, S., and S.A. Nelson, 2006. Correspondence analysis for detecting land cover change, *Remote Sensing of Environment*, 102:306–317.

Carr, J.R., and K. Matanawi, 1999. Correspondence analysis for principal components transformation of multispectral and hyperspectral digital images, *Photogrammetric Engineering & Remote Sensing*, 65(8):909–314.

Chavez, P.S., Jr., and A.Y. Kwarteng, 1989. Extracting spectral contrast in Landsat Thematic Mapper image data using selective principal component analysis, *Photogrammetric Engineering & Remote Sensing*, 55(3):339–348.

Chavez, P.S., Jr., S.C. Sides, and J.A. Anderson, 1991. Comparison of three different methods to merge multiresolution and multispectral: Landsat TM and SPOT Panchromatic, *Photogrammetric Engineering & Remote Sensing*, 57(3):295–303.

Chen, Y., T. Fung, W. Lin, and J. Wang, 2005. An image fusion method based on object-oriented image classification, *Proceedings of the Geoscience and Remote Sensing Symposium, IGARSS '05*, 6:3924–3927.

Cliche, G., F. Bonn, and P. Teillet, 1985. Integration of the SPOT pan channel into its multispectral mode for image sharpness enhancement, *Photogrammetric Engineering & Remote Sensing*, 51(3):311–316.

Ehlers, M., 1991. Multisensor image fusion techniques in remote sensing, *ISPRS Journal of Photogrammetry and Remote Sensing*, 46(1):19–30.

Gauch, H.G., Jr., 1982. *Multivariate Analysis in Community Structure*, Cambridge University Press, Cambridge.

Greenacre, M.J., 1984. *Theory and Application of Correspondence Analysis*, London, Academic Press.

Hill, M.O., 1974. Correspondence analysis: A neglected multivariate method, *Applied Statistics*, 23(3):340–354.

Hirschfield, H.O., 1935. A connection between correlation and contingency, *Proceedings of the Cambridge Philosophical Society*, 31:520–524.

Kroll, C., and Stedinger, J., 1996. Estimation of moments and quantiles using censored data, *Water Resources Research*, 32(4):1005–1012.

Laben, C.A., and B.V. Brower, 2000. *Process for Enhancing the Spatial Resolution of Multispectral Imagery Using Pan-sharpening*, United States Patent 6,011,875, Eastman Kodak Company, Rochester, New York.

Legendre, P, and L. Legendre, 1998. *Numerical Ecology*, Second English edition, Elsevier Science B.V., Amsterdam, 823 p.

Lemeshewsky, G.P., 1999. Multispectral multisensor image fusion using wavelet transforms, *Visual Image Processing VIII* (S.K. Park and R. Juday, Editors), Proceedings of SPIE, 3716:214–222.

Ling, Y., M. Ehlers, E.L. Usery, and M. Madden, 2007. FFT-enhanced IHS transform method for fusing high-resolution satellite images, *ISPRS Journal of Photogrammetry and Remote Sensing*, 61: 381–392.

Liu, J.G., 2000. Smoothing filter-based intensity modulation: A spectral preserve image fusion technique for improving spatial details, *International Journal of Remote Sensing*, 21(18):3461–3472

Liu, J.G., and J.M. Moore, 1998. Pixel block intensity modulation: Adding spatial detail to TM band 6 thermal imagery, *International Journal of Remote Sensing*, 19(13):2477–2491.

Pohl, C., and V. Genderen, 1998. Multisensor image fusion in remote sensing: Concepts, methods and applications, *International Journal of Remote Sensing*, 19(5):823–854.

Price, J.C., 1987. Combining panchromatic and multispectral imagery from dual resolution satellite instruments, *Remote Sensing of Environment*, 21(9):119–128.

Ranchin, T., and L. Wald, 2000. Fusion of high spatial and spectral resolution images: The ARSIS concept and its implementation, *Photogrammetric Engineering & Remote Sensing*, 66(1):49–61.

Ranchin, T., B. Aiazzi, L. Alparone, S. Baronti, and L. Wald, 2003. Image fusion-The ARSIS concept and some successful implementation schemes, *ISPRS Journal of Photogrammetry & Remote Sensing*, 58:4–18.

Shettigara, V.K., 1992. A generalized component substitution technique for spatial enhancement of multispectral images using a higher resolution data set, *Photogrammetric Engineering & Remote Sensing* 58(5):561–567.

Siddiqui, Y., 2003. The modified IHS method for fusing satellite imagery, *Proceedings of the ASPRS Annual Conference*, May, Anchorage, Alaska, unpaginated CD-ROM.

Švab, A., and K. OŠtir, 2006. High-resolution image fusion: Methods to preserve spectral and spatial resolution, *Photogrammetric Engineering & Remote Sensing*, 72(5):565–572.

Wald, L., T. Ranchin, and M. Mangolini, 1997. Fusion of satellite images of different resolutions: Assessing the quality of resulting images, *Photogrammetric Engineering & Remote Sensing*, 63(6):691–699.

Wald, L., 2002. *Data Fusion: Definitions and Architectures – Fusion of Images of Different Spatial Resolutions*, Les Presses, Ecole des Mines de Paris, Paris, France, 200 p.

Wang, Z., and A.C. Bovik, 2002. A universal image quality index, *IEEE Signal Processing Letters*, 9(3):81–84.

Welch, R., and M. Ehlers, 1987. Merging multiresolution SPOT HRV and Landsat TM data, *Photogrammetric Engineering & Remote Sensing*, 53(3):301–303.

Yesou, H., Y. Besnus, and J. Rolet, 1993. Extraction of spectral information from Landsat TM data and merger with SPOT panchromatic imagery – A contribution to the study of geological structures, *ISPRS Journal of Photogrammetry and Remote Sensing*, 48(5):23–36.

Zhang, Y., 1999. A new merging method and its spectral and spatial effects, *International Journal of Remote Sensing*, 20(10):2003–2014.

Zhang, Y., 2004. Understanding image fusion, *Photogrammetric Engineering & Remote Sensing*, 70(6):657–661.

Zhou, J., D.L. Civco, and J.A. Silander, 1998. A wavelet transform method to merge Landsat TM and SPOT panchromatic data, *International Journal of Remote Sensing*, 19(4):743–757.